

# High Speed Measurements of Flow Fields of a Series of Turbulent Premixed and Stratified Methane/Air Flames

Ruigang Zhou<sup>\*</sup>, Saravanan Balusamy, Simone Hochgreb  
Department of Engineering, University of Cambridge, CB2 1PZ, United Kingdom

## 1 Introduction

Fuel-lean, premixed combustion offers low NO<sub>x</sub> emissions and high fuel efficiency for many combustion devices [1, 2, 3]. Stratified mixtures with non-uniform fuel concentration, can yield better flame stability and ignitability compared with premixed flames under very fuel lean conditions [3, 4], and are often intentionally used in practical combustion systems, e.g. stratified charge engines.

Despite widespread use, there is still an incomplete understanding of how stratified flames behave relative to premixed flames at the fundamental level. This has motivated recent research on the effect of stratification on flammability limits [5], flame propagation speed [5, 6], flame surface density [7, 8, 9], flame brush thickness [7, 9, 10], scalar dissipation rate [9] and curvature [7, 8, 9, 11], as well as flame structure [12, 13].

A number of recent experimental studies have examined results from novel turbulent stratified burners at practically relevant turbulence levels [8, 14, 15, 16, 17]. The present work uses high speed stereo particle image velocimetry (HS-SPIV) and laser Doppler anemometry (LDA) to investigate the flow fields from methane/air flames in a turbulent swirl burner, described previously in [12, 13]. Previous measurements of temperature, major species (CO, H<sub>2</sub>, CO<sub>2</sub>, H<sub>2</sub>O, CH<sub>4</sub>, O<sub>2</sub> and N<sub>2</sub>), three-dimensional thermal gradients, and curvature of these flames have been acquired using Raman/Rayleigh/CO-LIF combined with simultaneous cross-planar OH-PLIF techniques. The motivation for the present work is to characterize the flow field of the burner with high temporal resolution, provide a complete velocity database for modelling researchers, and investigate the effect of heat release, stratification and swirl on the flow fields of the burner.

## 2 Experimental details

An overview of the burner, operating conditions, and experimental set up is provided in this section.

### 2.1 Cambridge/Sandia Stratified Swirl Burner

The burner, denoted as the *Cambridge/Sandia Stratified Swirl Burner*, was designed to provide flows with a variable degree of fuel stratification as well as swirl; this was to approximate the flow conditions found in many practical applications, and to introduce a greater degree of complexity to the test case. The swirl assists flame stabilization, as in practical combustors, allowing more extreme stratified conditions to be investigated.

The geometry of the swirl burner is detailed in Figure 1. The burner is formed from co-annular tubes with a development length exceeding 25 hydraulic diameters to ensure well developed turbulent flow. A ceramic central bluff body is used to stabilize the flame with minimal heat loss. The geometry is described in detail in [12]. The inner annulus equivalence ratio ( $\phi_i$ ) and the outer annulus equivalence ratio ( $\phi_o$ ) were independently controlled using mass flow controllers, allowing the stratification ratio ( $SR = \phi_i/\phi_o$ ) to be easily varied. The swirl flow ratio ( $SFR$ ), defined as the ratio of outer annulus flow passing through a swirl plenum relative to the total outer annulus flow, could be independently set, enabling well defined and reproducible swirl levels.

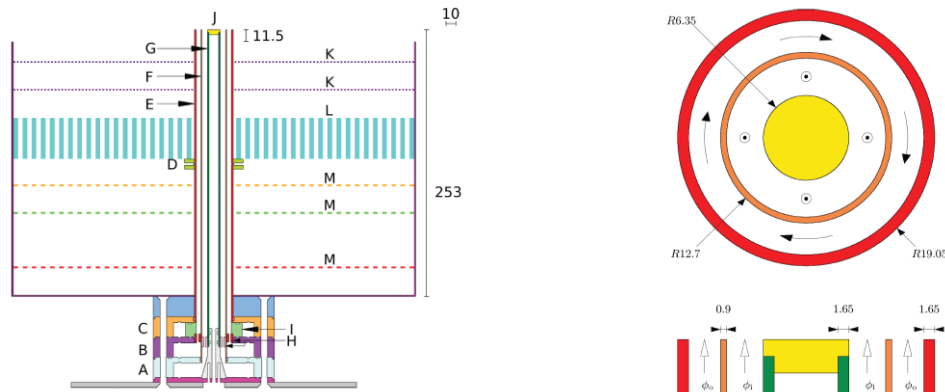


Figure 1. Burner geometry. Left: Cross-section of the burner. Right: Exit geometry of the burner.

## 2.2 Operating Conditions

The operating conditions for the present study are shown in Table 1. The generalized notations  $cSwBN_z$  and  $SwBN_z$  are used to denote non-reacting and reacting cases respectively, where  $N$  is the case number and  $z$  is the downstream distance in millimetres; for example, the premixed non-swirling case at  $z = 30$  mm downstream of the burner exit is denoted  $SwB1_{30}$ .

Table 1: Operating conditions for Cambridge Stratified Swirl Burner.

Flame	$SFR$	$\phi_i$	$\phi_o$	$SR$	$\phi_g$	
$SwB1$	0%	0.75	0.75	1	0.75	
$SwB2$	25%					
$SwB3$	33%					
$SwB5$	0%	1	0.5	2		
$SwB6$	25%					
$SwB7$	33%					
$SwB9$	0%	1.125	0.375	3		
$SwB10$	25%					
$SwB11$	33%					
$cSwB1$	0%	Non-Reacting				
$cSwB2$	25%					
$cSwB3$	33%					

These conditions were chosen to allow the investigation of flames in premixed and stratified regimes, with or without swirl. The bulk velocity in the outer annulus,  $U_o = 18.7$  m/s, was set at more than twice the value of the velocity in the inner annulus,  $U_i = 8.3$  m/s, in order to generate substantial levels of shear between the two flows. Co-flow air was supplied around the outer annulus with a bulk velocity  $U_{co} = 0.4$  m/s to provide well-characterized boundary conditions. The Reynolds numbers derived from the bulk velocities at the exit geometry are  $Re_i = 5960$  for the inner flow and  $Re_o = 11500$

for the outer flow. The stratification ratio was varied from 1 for premixed cases to 3 for the most stratified cases. The swirl flow ratio was varied between 0 for non-swirling flow to 33% for highly swirling flow.

### 2.3 HS-SPIV configuration

The velocity characterization was performed using HS-SPIV first, giving the velocity components in the axial, radial and tangential directions. The inner flow, outer flow, and co-flow were each seeded with 1  $\mu\text{m}$  calcined aluminium oxide particles. The seeding was achieved by passing a portion of each air flow through turbulent fluidized seeders, and adjusting the fraction of the total flow through each seeder with needle valves to ensure similar seed density in all streams. The particles were illuminated using a New Wave Research Pegasus-PIV system. The system consists of a dual-head, high repetition rate Nd:YLF laser, two LaVision CCD cameras (FASTCAM Ultima APX), and a high speed controller (LaVision) interfaced with a computer through DaVis software. The laser delivers pulses of 527 nm wavelength with 4.5 mJ energy per pulse at 3 kHz. Laser sheet of 1 mm in thickness is created by two cylindrical lenses. CCD cameras are equipped with Scheimpflug adapters and Nikon AF micro Nikkor 60 mm lenses (f/2.8). Mie scattering images are acquired at 3 kHz, which is the maximum repetition rate achievable with 605 pixel  $\times$  516 pixel image size, and 61.7 mm wide by 52.0 mm tall image area. For each case, 4096 PIV image pairs are acquired. The time delay between each pulse is optimized to 10  $\mu\text{s}$  based on the interrogation window size and maximum displacement of particles pair to be within  $1/3^{\text{rd}}$  of interrogation window size.

The images were processed using LaVision software (DaVis 7.4). Raw images were pre-processed by subtracting a sliding background (3 pixel scale length) and normalizing the particle intensity using a min/max filter (3 pixel scale length). Vectors were calculated using multi-pass cross-correlation with an initial window size of 32  $\times$  32, decreasing to a 12  $\times$  12 window size in the final three passes. The window overlap was held constant at 50% in each pass. This gives a vector spatial resolution of 0.61 mm/vector. Vectors where the Q-factor (ratio of highest to second highest peaks in the displacement correlation map) was below 1.2 were eliminated. The resulting fields were median filtered.

### 2.4 Pairwise LDA configuration

The present LDA configuration is a conventional system from Dantec. A brief overview of set up is present here and details can be found in [18]. The laser used is an Ar-ion continuous laser (Spectra-Physics Stabilite 2017) operating at 514.5 nm and 488 nm with power set to 1.5 W. The signals generated by the particles were transferred to the BSA processor through a Nikon Micro Nikkor 105 mm lens (f/2.8), a pinhole, a Dantec colour separator and photodetectors operating at 514.5 nm and 488 nm, giving the measurements of the first and second velocity components. A pairwise LDA set up was achieved by rotating the system by 90 degrees and scanning along the same positions to obtain the third velocity component. As a result all three velocities, axial, radial and tangential, are resolved at the measurement locations with at least 10 kHz data rate. Radial symmetry of the flows is ensured by acquiring full radial scans. The measurements were taken at multiple axial locations, corresponding to previous publications regarding the scalar measurements [12, 13].

## 3 Results and discussion

### 3.1 Flow Patterns

This section presents the general flow patterns derived from the PIV data for all operating conditions. Maps of mean velocity,  $\bar{U} = \sqrt{\bar{u}^2 + \bar{v}^2 + \bar{w}^2}$ , and fluctuating velocity  $U' = \sqrt{u'^2 + v'^2 + w'^2}$ , are shown in Figure 2.  $\bar{U}$  and  $U'$  are shown only from the same half of the domain as radial symmetry of the profiles has been obtained.  $\bar{U}$  shown at  $r < 0$  mm is mirrored from profiles of  $r > 0$  mm while  $U'$  is shown for  $r > 0$  mm. Streamlines are shown in black to highlight the flow patterns.

The flow fields, whether reacting or not, demonstrate features typical of co-annular jet flow with a central bluff body: the peak velocities are found between the annuli with recirculation zones formed

over the bluff body. The effect of shear layers on turbulence are evident in the images for  $U'$  between the recirculation zone, the inner flow, the outer flow, and the co-flow.

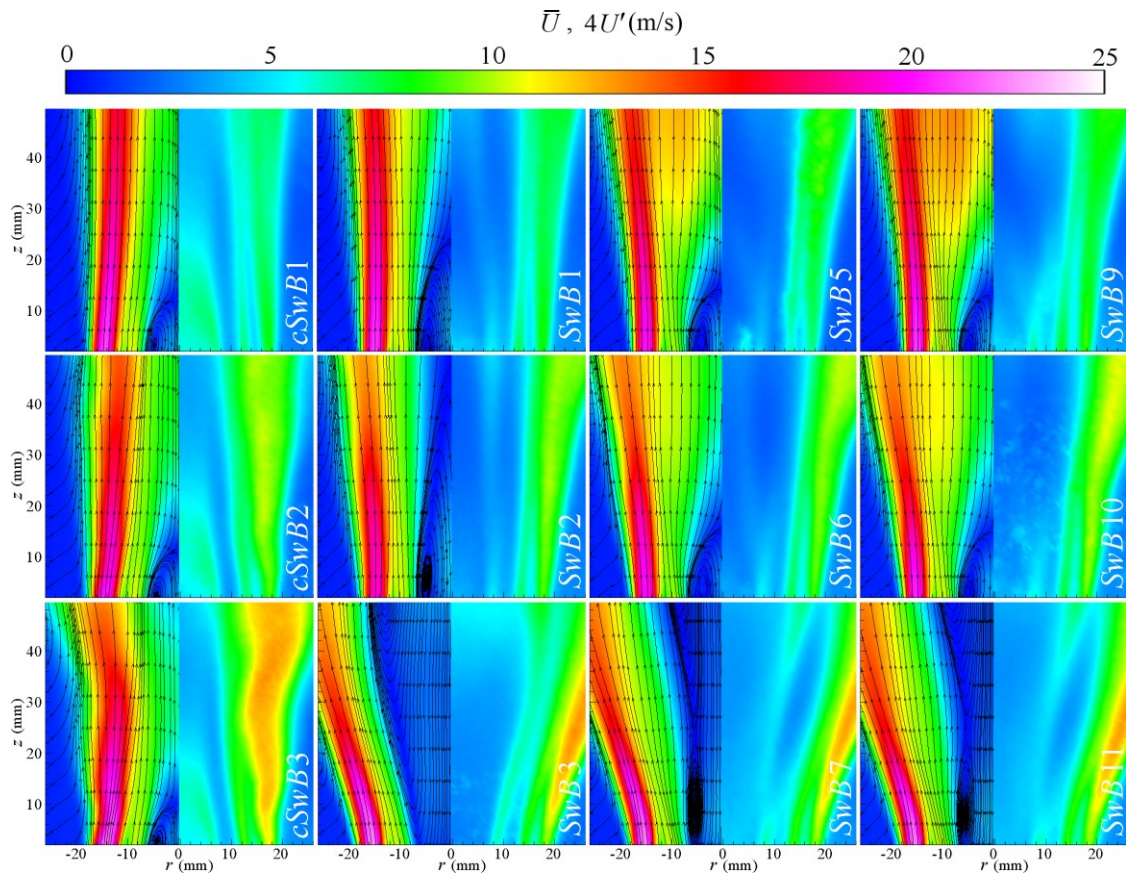


Figure 2. Mean ( $r < 0$  mm) and fluctuating ( $r > 0$  mm) velocities for non-swirling (top row), moderately swirling (middle row) and highly swirling (bottom row) flows. Columns from left to right correspond to non-reacting, premixed, moderately stratified and highly stratified states. Streamlines are shown in black for  $r < 0$  mm.

The behaviour of the recirculation zone above the central bluff body varies substantially depending on whether or not the flow is reacting, the stoichiometry, and the degree of swirl. The non-reacting cases exhibit a narrow recirculation zone typical of annular axial flows past a flat central bluff body. The swirl significantly increases the intensity of turbulent fluctuations. The recirculation zone is long and thin in the premixed cases, and more compact in the stratified cases, forming a waist on the streamlines where the top of the recirculation zone meets the diverging flow field. The effects of stratification accentuate the pattern: the premixed  $SwB3$  forms a primary conically shaped recirculation zone with the centre farther downstream, while the stratified cases ( $SwB7$  and  $SwB11$ ) show signs of secondary conically shaped recirculation zones in the downstream region where the difference in stoichiometries disappears due to inter-stream mixing.

The flows in the reacting cases move radially outwards relative to non-reacting flows due to the expansion of the hot products; the effect is more pronounced in the stratified cases due to the higher equivalence ratios and corresponding higher temperatures in the inner region of the flow field. The turbulence intensity within the recirculation zones is suppressed by combustion due to increases in the kinematic viscosity and subsequently dissipation of turbulence.

### 3.2 HS-SPIV vs. Pairwise LDA

#### 3.2.1 Mean and Fluctuating Velocity

Figure 3 shows the comparison between HS-SPIV and Pairwise LDA radial profiles of mean and fluctuating velocity for non-reacting and reacting cases at axial location  $z = 30$  mm.

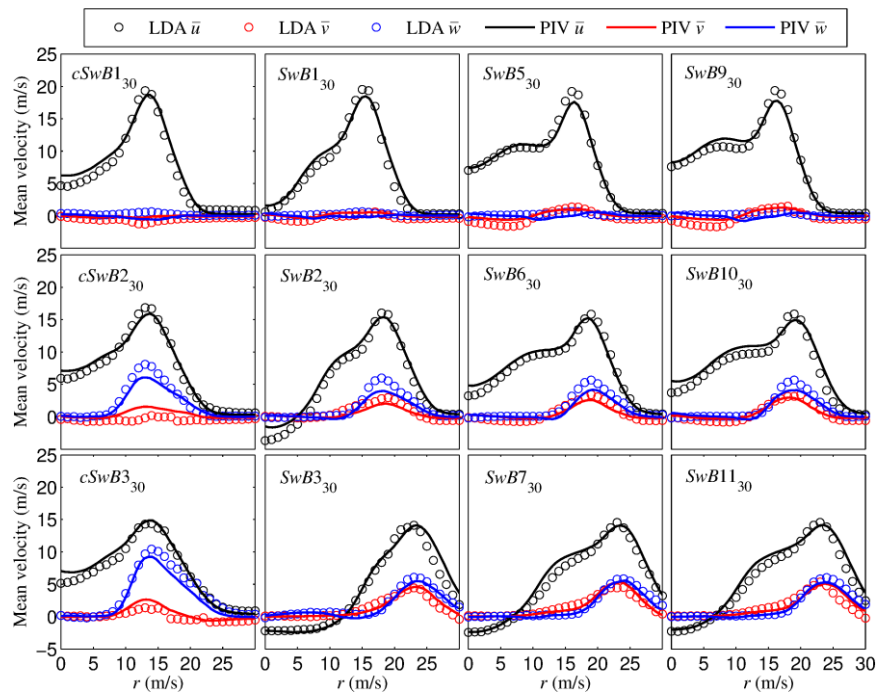


Figure 3. Radial profiles of mean axial velocity for all non-reacting and reacting cases, extracted at  $z = 30$  mm from HS-SPIV and Pairwise LDA.

The results show remarkably good agreement, in spite of any differences in operating principle, burner alignment, and spatial as well as temporal resolutions.

### 3.2.2 Power Spectral Density and Auto Correlation Function

The power spectral density (*PSD*) and autocorrelation function (*ACF*) derived from HS-SPIV and LDA data are compared and shown in Figure 4. The present study used a sample-and-hold reconstruction method to create equidistantly spaced time series, thereby allowing a *FFT* to be used for *PSD* estimation. The *ACF* is obtained by applying inverse *FFT* to the *PSD*. Details on the optimization of the estimations of *PSD* and *ACF* are available in [18].

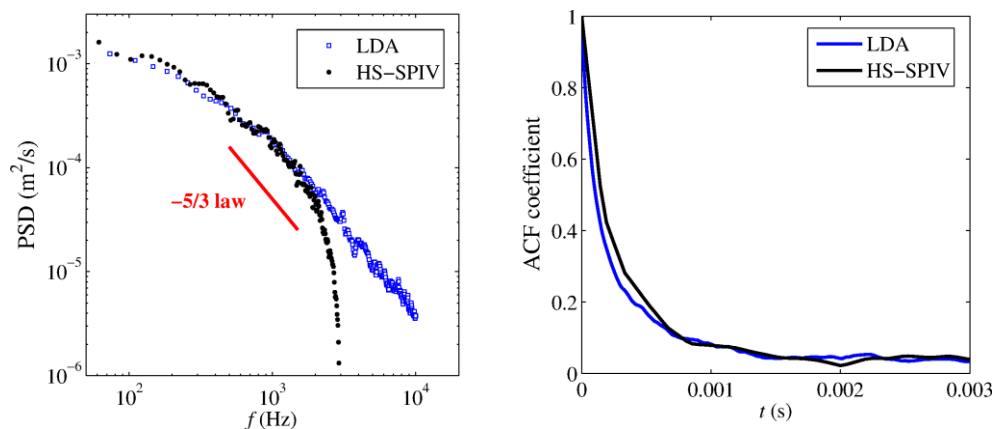


Figure 4. Comparisons of LDA and PIV in terms of *PSD* (left) and *ACF* (right) for case  $cSwB1_{10}$  at  $r=9$  mm.

The cut-off frequency for the HS-SPIV measurements is 1500 Hz according to the Nyquist criterion, and the limit clearly shows in the fall-off curve for the *PSD*. The agreement in the slow time/large spatial scales is good, and the LDA measurements demonstrate the expected decay of the

turbulence with a  $-5/3$  power decay towards the small scales. The *ACFs* of HS-SPIV and LDA are also in good agreement, suggesting similar turbulence parameters to be obtained using these two different techniques.

## 4 Concluding remarks

The present study provides an accurate database for the flow field of the *Cambridge/Sandia Stratified Swirl Burner* by using two different techniques: HS-SPIV and Pairwise LDA. Results obtained from HS-SPIV and Pairwise LDA are compared and show an excellent agreement in terms of mean and fluctuating velocity as well as power spectral density and autocorrelation function.

The flow patterns demonstrate features typical of co-annular jet flow with a central bluff body: the peak velocities are found between the annuli, with recirculation zones formed over the bluff body. The reacting flows move radially outwards relative to non-reacting flows due to the expansion of the hot products; the effect is more pronounced in the stratified cases due to the higher equivalence ratios and corresponding higher temperatures experienced in the inner regions. The difference in fuel distribution also leads to substantial change in the recirculation zones for highly swirling cases: the premixed flame forms a primary conically shaped recirculation zone with the centre at farther downstream, while the stratified flames show signs of secondary conically shaped recirculation zones further downstream where the mixture stratification disappears due to turbulent diffusion. The fuel distribution effects interact significantly with swirl: the recirculation zones are more compact under stratified conditions whereas they are elongated under premixed conditions.

## References

- [1] K. H. Lyle, L. K. Tseng, J. P. Gore, N. M. Laurendeau, *Combust. Flame* 126 (1999) 627-639
- [2] S. Shiga, S. Ozone, H. T. C. Machacon, T. Karasawa, H. Nakamura, T. Ueda, N. Jingu, Z. Huang, M. Tsue, M. Kono, *Combust. Flame* 129 (2002) 1-10.
- [3] A. C. Alkidas, *Energy Convs. Manage.* 48 (2007) 2751-2761.
- [4] Y. Li, H. Zhao, B. Leach, T. Ma, *Proc. IMechE Part D: J. Automobile Engineering* 219 (2005) 923-934.
- [5] T. Kang, D. C. Kyritsis, *Proc. Combust. Inst.* 23 (2007) 1075-1083.
- [6] N. Pasquier, B. Lecordier, M. Trinite, A. Cessou, *Proc. Combust. Inst.* 31 (2007) 1567-1574.
- [7] P. Anselmo-Filho, S. Hochgreb, R. S. Barlow, R. Cant, *Proc. Combust. Inst.* 32 (2009) 1763-1770.
- [8] P. C. Vena, B. Deschamps, G. J. Smallwood, M. R. Johnson, *Proc. Combust. Inst.* 33 (2011) 1551-1558.
- [9] M. S. Sweeney, S. Hochgreb, R. S. Barlow, *Combust. Flame* 158 (2011) 935-948.
- [10] B. Renou, E. Samson, A. Boukhalfa, *Combust. Sci. Tech.* 176 (2004) 1867-1890.
- [11] V. Robin, A. Mura, M. Champion, O. Degardin, B. Renou, M. Boukhalfa, *Combust. Flame* 153 (2008) 288-315.
- [12] M. S. Sweeney, S. Hochgreb, M. J. Dunn, R. S. Barlow, *Combust. Flame* 159 (9) (2012) 2896-2911.
- [13] M. S. Sweeney, S. Hochgreb, M. J. Dunn, R. S. Barlow, *Combust. Flame* 159 (9) (2012) 2912-2929.
- [14] F. Seffrin, F. Fuest, D. Geyer, A. Dreizler, *Combust. Flame* 157 (2) (2010) 384-396.
- [15] B. Böhm, J. H. Frank, A. Dreizler, *Proc. Combust. Inst.* 33 (1) (2011) 1583-1590.
- [16] M. S. Sweeney, S. Hochgreb, M. J. Dunn, R. S. Barlow, *Proc. Combust. Inst.* 33 (2011) 1419-1427.
- [17] C. Galizzi, D. Escudié, *Combust. Flame* 157 (12) (2010) 2277-2285.
- [18] R. Zhou, M. S. Sweeney, S. Hochgreb, R. S. Barlow, *Flow Field Studies of A Series of Turbulent Premixed and Stratified Methane/Air flames*, *Combustion and Flame* (2012), *submitted*